⌘ *Author's Choice*

Interactions between the Yeast SM22 Homologue Scp1 and Actin Demonstrate the Importance of Actin Bundling in Endocytosis*⑤

Dana M. Gheorghe[‡1], **Soheil Aghamohammadzadeh**[‡2], **Iwona I. Smaczynska-de Rooij**[‡3], **Ellen G. Allwood**[‡], **Steve J. Winder**[§], and **Kathryn R. Ayscough**[‡4]

From the Departments of ‡Molecular Biology and Biotechnology, §Biomedical Science, University of Sheffield, Sheffield, S10 2TN, United Kingdom

The yeast SM22 homologue Scp1 has previously been shown to act as an actin-bundling protein *in vitro*. In cells, Scp1 localizes to the cortical actin patches that form as part of the invagination process during endocytosis, and its function overlaps with that of the well characterized yeast fimbrin homologue Sac6p. In this work we have used live cell imaging to demonstrate the importance of key residues in the Scp1 actin interface. We have defined two actin binding domains within Scp1 that allow the protein to both bind and bundle actin without the need for dimerization. Green fluorescent protein-tagged mutants of Scp1 also indicate that actin localization does not require the putative phosphorylation site Ser-185 to be functional. Deletion of *SCP1* has few discernable effects on cell growth and morphology. However, we reveal that *scp1* deletion is compensated for by up-regulation of Sac6. Furthermore, Scp1 levels are increased in the absence of *sac6.* The presence of compensatory pathways to up-regulate Sac6 or Scp1 levels in the absence of the other suggest that maintenance of sufficient bundling activity is critical within the cell. Analysis of cortical patch assembly and movement during endocytosis reveals a previously undetected role for Scp1 in movement of patches away from the plasma membrane. Additionally, we observe a dramatic increase in patch lifetime in a strain lacking both *sac6* and *scp1*, demonstrating the central role played by actin-bundling proteins in the endocytic process.

The actin cytoskeleton plays a key role in cell organization to facilitate processes such as motility, cell polarity, and membrane trafficking. In yeast, as in other eukaryotes, actin functions primarily in its filamentous form, F-actin. Dynamic rearrangements of F-actin are critical to allow a cell to carry out its functions, and these are controlled by a number of proteins that regulate polymerization and depolymerization of the filament. Budding yeast expresses most classes of actin-binding proteins including profilin, cofilin, tropomyosin, capping protein, Arp2/3, and formins (1). The formins Bni1 and Bnr1 are required for the generation of long filaments that are bundled by the fimbrin homologue Sac6p into actin cables. These cables are directional, forming at the bud tip or neck region, and are important for polarized movement of secretory vesicles to ensure growth occurs primarily in the bud. The other main actin-containing structures in yeast cells are cortical actin patches. These contain a plethora of actin binding and regulatory proteins, indicating the importance of rapid assembly and disassembly of actin filaments that must take place at these sites. Actin patches are now considered to represent a stage of endocytic vesicle formation (for review, see Refs. 2 and 3). In brief, endocytic sites form through recruitment of coat components such as clathrin and other proteins including Sla2 (homologue of mammalian Hip1R). The homologue of WASP, called Las17, is also recruited to these sites. Invagination of the membrane to form the endocytic vesicle is proposed to be brought about when actin is actively assembled via Las17 activation of Arp2/3 into filaments at these sites. Attachment between actin-binding proteins and endocytic coat proteins couples actin polymerization to the inward movement of membrane, and the membrane is pulled into the cell. Recruitment of amphiphysin homology proteins Rvs161 and Rvs167 to the neck of the vesicle is then thought to play a role in its scission.

Both Sac6 and a homologue of mammalian SM22/transgelin, Scp1, have been shown to be capable of bundling actin *in vitro*, and both localize to the cortical actin patches (4, 5). Deletion of *sac6* has marked effects on cell growth, and its role in stabilizing actin cables as well as within patches could partly explain this more severe phenotype (6, 7). Δ*sac6* cells were also reported to have a defect in endocytic uptake of the pheromone α-factor (8). Deletion of *scp1* on the other hand has not been reported to have observable actin defects in a wild-type cell background, although its deletion does increase cell longevity, an effect proposed to be due to increased actin dynamics (9). Additionally, in combination with a *sac6* deletion, there is an additive effect, with very disorganized actin patches and cables, suggesting that the two proteins may play a partially overlapping role in stabilizing actin in the cortical patches (4, 5). More recently, a study

aimed at investigating the behavior of endocytic patches found that in Δ*sac6* cells many of the patches were aberrant in their movement away from the membrane (10). These data suggested a model in which Sac6 could bundle actin during the invagination processes to provide a strong framework to allow sufficient force to be generated to pull the membrane into the cell. Although the data on Sac6 strongly support the idea of bundling being important for the invagination process, questions then arise as to the role for a second bundling protein that apparently functions in the same place and at the same time as Sac6. Why does the cell express two bundling proteins that function during the same process? In this study we aimed to investigate Scp1 further to determine how it interacts with actin and whether it plays a role distinct to that of Sac6 in its organization of actin. We use both biochemical analysis and cell imaging to identify regions in actin and within Scp1 that are important for their interaction. We investigate endocytic patch assembly in cells lacking either *sac6*, *scp1*, or both of these bundling proteins and reveal a role for Scp1 in formation and movement of endocytic patches. Our data also suggest that actin organization by Sac6 and Scp1 *in vivo* are distinct, with Scp1 likely to form tighter bundles and function at a later stage of endocytosis than Sac6.

EXPERIMENTAL PROCEDURES

Yeast Strains and Cell Growth—Yeast strains used in this study are listed in supplemental Table 1. Yeast were grown with rotary shaking in liquid YPD medium (1% yeast extract, 2 Bacto-peptone, 2% glucose supplemented with 40 μg/ml adenine) or in synthetic medium 0.67% yeast nitrogen base, 2% glucose with appropriate supplements to maintain plasmids as required (Sigma-Aldrich). Transformations were performed using lithium acetate as previously described (11). Genomic deletion of *sac6*, RFP[5] tagging of Abp1, and truncations of Scp1were carried out using the PCR knock-in strategy (12) and verified using PCR of genomic DNA. Overexpression was carried out using previously generated plasmids pKA280 and pKA281 that were transformed in wild-type and *act1–102* strains (5). Overexpression was induced by plating on synthetic medium agar plates lacking methionine.

In vitro mutagenesis was used to generate Scp1 mutant plasmids. Plasmids and oligonucleotides primers are as described in supplemental Tables 2 and 3. Mutagenesis was carried out using the Stratagene QuikChange kit according to the manufacturer's instructions and using oligonucleotides listed in supplemental Table 3.

Protein Purification and Assays—Scp1 was purified as described previously (5) by expression of *SCP1* from pKA211 in *Escherichia coli* BL21(DE3) cells. In addition, His$_6$-tagged Scp1 and Scp1-(1–180) were generated (pKA501 and pKA491, respectively) and purified on nickel-agarose according to the manufacturer's instructions (Qiagen).

Yeast actin was purified as described (13). Rabbit skeletal muscle actin was purified as described previously (14). G-actin (mammalian or yeast) was pre-polymerized overnight at 4 °C or

for 2 h at room temperature with $10\times$ KME buffer (0.1 M Tris-HCl, pH 8.0, 0.5 M KCl, 10 mM MgCl$_2$, 10 mM EGTA, added as 1/10 of the total sample volume), then Scp1p was added to the samples and allowed to bind to the actin filaments for 10 min. The samples were then spun at $20,500 \times g$ (low speed assay) or at $350,000 \times g$ (high speed assay) for 30 min at 4 °C in a Beckman TLA100 rotor. The pellet fractions were resuspended in G-buffer of an equal volume to that of the supernatant (50 or 100 μl), then both pellet and supernatant fractions were mixed with $2\times$ sample buffer (50 or 100 μl). The samples were run on a 12% SDS-PAGE gel, the gels were Coomassie-stained and destained, and the integrated densities of the bands obtained were quantified using the NIH Image 1.61 software.

Fluorescence Microscopy—Fluorescence microscopy for live cell imaging was performed with a DeltaVision RT Restoration Microscopy System running SoftWoRx™ image analysis and model-building application (Applied Precision Instruments, Seattle, WA). Cells expressing tagged proteins were visualized after growing to early log phase in synthetic medium with appropriate supplements. All image data sets were deconvolved, the distance of moving fluorescence spots were measured, and the arbitrary profile of intensity values, image coordinates, and tracking of patch movements were established using the SoftWoRx application. Images were exported as TIFF files, and image size was adjusted to 300 dpi and assembled using Adobe Photoshop CS2. Kymographs were assembled in ImageJ. For patch diameters, kymographs were assembled, and the patch diameter was measured at the point immediately before movement away from the membrane. To visualize and capture images of Abp1RFP and GFP5-Scp1 simultaneously, a Dual View system (Optical Insight, Tucson, AZ) was used.

Immunofluorescence microscopy was used to visualize Sac6 following fixation with formaldehyde and treatment of cells with methanol and acetone as described (15). Sac6 antibodies were a gift from D. Drubin (U.C. Berkeley) and were used at a dilution of 1:100. Cells were visualized on an Olympus BX-60 microscope, and images were captured with a MicroMax 1400 CCD camera (Roper Scientific) using Scanalytics software on a Mac7300 computer.

Rhodamine-phalloidin staining was performed as described (16). Lucifer yellow staining was performed as described by Dulic (17) except that staining was for 80 min. Images were recorded as described above.

RESULTS

Mapping of the Scp1 Binding Site on Actin—Previous studies have demonstrated that binding sites for both drugs and proteins on actin can be mapped *in vivo* by the use of mutant actin alleles (18–20). 16 yeast strains, each expressing a different mutant allele of actin (in the absence of wild-type actin), were transformed with a GFP-Scp1 plasmid (4, 5). Localization of Scp1 was determined in each case. Two plasmids were used, one where Scp1 was overexpressed from a heterologous (galactose) promoter (5) and one in which Scp1 was expressed from its own promoter (4). In both cases the data are qualitatively similar, and only the data for expression from its own promoter are shown. Fig. 1*A* shows the localization in wild type and a number of the mutant alleles. Of the 16 strains, 3 showed sig-

---

[5] The abbreviations used are: RFP, red fluorescent protein; GFP, green fluorescent protein.
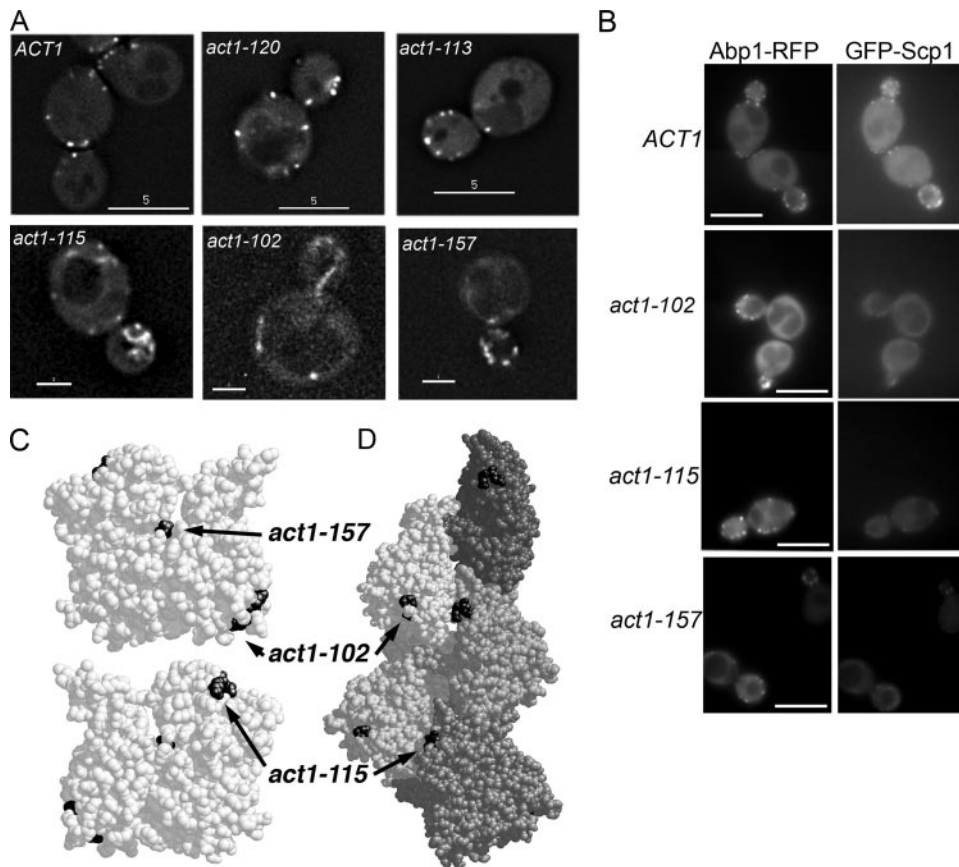
FIG. 1. **Localization of GFP-Scp1 in strains expressing different actin alleles.** *A*, GFP-Scp1 was expressed in wild-type cells and 16 strains expressing different actin alleles (Table 1). Three of these, *act1–102*, *act1–157*, and *act1–115*, showed markedly reduced localization of GFP-Scp1 when compared with wild-type and other mutant strains. *Act1–120*-expressing strains do not localize Sac6, the other actin bundling protein of cortical patches, but do localize Scp1. *Act1–113*-expressing strains localize GFP-Scp1 in a similar way to wild-type cells. *Bar*: 5 μm (*upper panels*); 2 μm, (*lower panels*). Exposure times: 3 s for *ACT1*, *act1–113*, and *act1–120*; 5 s for *act1–102*, *act1–115*, and *act1–157*. *B*, to verify Scp1 patches localization, strains expressing Abp1-mRFP and GFP-Scp1 were generated. RFP and GFP were imaged simultaneously for 1 s to allow comparison between intensities to be facilitated. *Bar*, 5 μm. *C*, localization of the three non-localizing mutants on the actin monomer. *D*, localization of the three non-localizing alleles on the modeled actin filament. Note the position of *act1–115* at the filament interface. *Act1–102* is the most accessible of the three sites and is likely to represent one of the Scp1 binding sites on actin.

nificantly reduced Scp1 localization to cortical actin patches (Fig. 1; Table 1). To confirm whether the patches visible in these mutants were indeed associated with actin, we generated strains that also expressed the well characterized F-actin-binding protein Abp1 fused with mRFP. Localization of Abp1-mRFP and GFP-Scp1 was recorded simultaneously using a DualView beamsplitter using the same exposure time of 1 s. As shown in Fig. 1*B*, Abp1-mRFP is clearly visible in cortical patches as is GFP-Scp1 in cells expressing wild-type actin. In each of the actin mutants Scp1 does co-localize to Abp1-containing spots but with a markedly reduced level of intensity. We also stained the three mutant alleles with reduced Scp1 localization with rhodamine phalloidin (supplemental Fig. 1). These data indicate that *act1–102* and *act1–157* strains have an actin staining pattern indistinguishable from that of actin, suggesting that the actin in these cells is fully capable of forming filaments and organizing these appropriately. Actin organization in *act1–115*-expressing cells is more aberrant with no clear long cables and with non-polarized actin patches. This organization may

suggest that actin in these cells is more dynamic and less well able to form stable structures such as cables.

The position of the three allele mutations within the monomer is shown in Fig. 1*C* and within a model filament in Fig. 1*D*. The mutations were distributed across the monomer with, at first glance, no clear region to mark a site of interaction. However, one of the alleles that shows a reduced level of localization, *act1–157*, actually resides in the ATP binding cleft (D157E), and we know this is unlikely to be accessible to binding. This mutant had been generated as part of a series of mutants that are affected in ATP binding dynamics, and in fact this mutant was demonstrated to have increased nucleotide exchange and filament turnover (21). We postulated that as an actin bundling protein, Scp1, might bind preferentially to more stable actin, and if the levels of this are reduced in these cells due to increased actin turnover, this would explain the reduced actin association.

The mutations in *act1–115* lies close to the actin-actin interface within the filament, and the two residues mutated (E195A and R196A) lie close to a loop that is believed to play an important role in stabilizing interfilament connections by forming a cross-filament bridge to a hydrophobic pocket (22). Furthermore, residues immediately adjacent (Gly-197—Thr-203) participate in longitudinal interactions between protomers in the same strand via both hydrogen bonds and van der Waals forces (23). Previously we have observed that despite this strain having relatively normal growth phenotypes, its actin is particularly susceptible to the effects of the actin monomer associating drug latrunculin-A, indicating that its actin is particularly dynamic or unstable (19). As with *act1–157*, we therefore postulate that the lack of binding in this case is due to the absence of sufficiently stable actin to allow Scp1 to bind rather than marking a *bona fide* binding site. The remaining mutant, *act1–102*, defined by mutations K359A and E361A, lies on the surface of the actin monomer in a region that is known to interact with a number of actin-binding proteins, and we, therefore, considered this as a likely binding sites for Scp1 on actin.

Because other actin binding proteins, Sac6 (yeast fimbrin) and Abp1, have been suggested to interact physically or genetically with Scp1, we also determined whether these proteins are able to localize in the *act1–102* mutant. As shown in Fig. 2, *A*

TABLE 1

Localization of GFP-Scp1 in strains expressing different actin alleles

| Actin allele	Mutations present	Location of mutations on monomer subdomains	Wild-type GFP-Scp1 localization
ACT1	None (wild type)		+
act1–133	D24A, D25A	I	+
act1–101	D363A, E364A	I	+
act1–102	K359A, E361A	I	−
act1–113	R210A, D211A	IV	+
act1–115	E195A, R196A	IV	−
act1–119	R116A, E117A, K118A	I	+
act1–120	E99A, E100A	I	+
act1–129	R177A, D179A	IV	+
act-45	I341A	I	+
act1–53	I345A	I	+
act1–54	Y166T	III	+
act1–57	I341K	I	+
act1–61	Y166A	III	+
act1–62	F169A	III	+
act1–63	Y166A, F169A	III	+
act1–157	D157E	Nucleotide binding cleft	−

Abp1-GFP
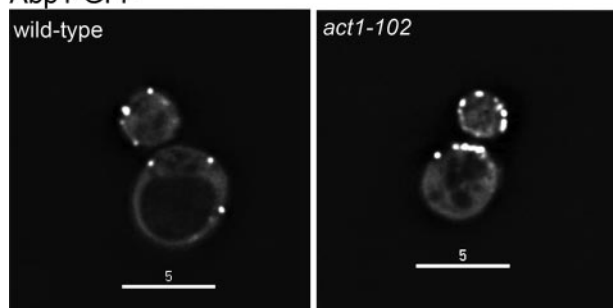
anti-Sac6
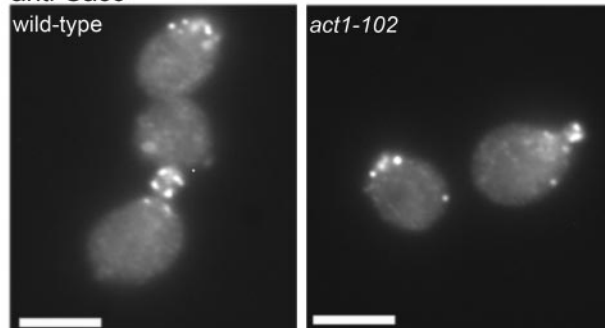
FIG. 2. Localization of Abp1 and Sac6 occurs normally in the *act1–102* strain. *A*, Abp1-GFP localizes to cortical actin patches in wild-type and in Δscp1 cells, demonstrating that Abp1 is not responsible for localizing Scp1 to actin *in vivo*. *Bar*, 5 μm. *B*, Sac6 was localized using immunofluorescence microscopy to cortical actin patches in both wild-type and *act1–102* cells, demonstrating that these bundling proteins have distinct interaction sites on actin. *Bar*, 5 μm.

and *B*, both Sac6p and Abp1 localize in a wild-type pattern in this mutant. Thus, althoughAbp1 has been reported to interact with Scp1, the presence of Abp1 on actin is not sufficient to recruit Scp1. In addition, although Sac6p and Scp1 have an apparently additive role in stabilizing actin in the endocytic cortical patches, they do not use completely overlapping actin binding sites. This was further confirmed in the mutant *act1–120* (Fig. 1*A*) in which Scp1 localizes as in wild-type cells but which is unable to localize Sac6 (20).

In previous studies we have shown that overexpression of Scp1 is detrimental and prevents growth on appropriate growth
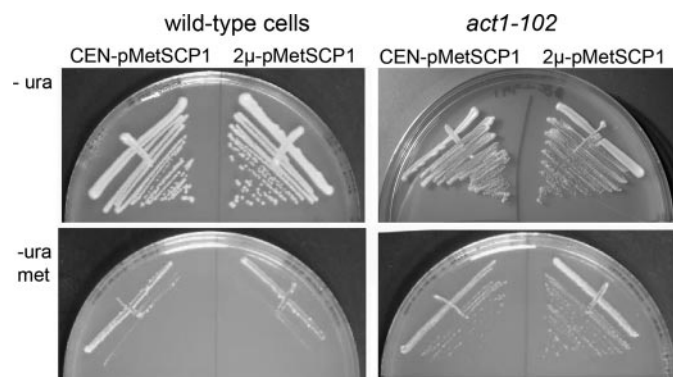

FIG. 3. Overexpression of *SCP1* is not lethal in the *act1–102* strain. *SCP1* was cloned behind a methionine promoter on a low copy number (centromeric) and high copy number (2μ) plasmid. Expression was induced when strains were plated on media lacking methionine. As shown in the *lower left panel*, wild-type cells cannot tolerate overexpression of Scp1. In contrast, *act1–102* cells are still able to grow in the presence of the overexpressing plasmid on plates lacking methionine, indicating that inviability caused by *SCP1* overexpression is due to its interaction with actin.

media that causes *SCP1* induction (5). We, therefore, reasoned that if Scp1 is unable to associate with actin in the *act1–102* strain and if actin bundling is the cause of cell death in the overexpressing cells, then Scp1 overexpression might no longer be lethal in *act1–102* cells. This was tested by transforming cells with a plasmid carrying *SCP1* which overexpresses the gene only when cells are placed on media lacking methionine. As shown in Fig. 3, whereas both wild-type and *act1–102* cells can grow in the presence of methionine, removal of this nutrient causes expression from the plasmid, and in the case of wild-type cells, this overexpression of *SCP1* leads to cell death. On the other hand, *act1–102* cells are able to grow in the presence of this higher level of Scp1, supporting the idea that the mutations in *act1–102* have disrupted the binding interface with Scp1 and demonstrating that actin binding is the cause of cell death when Scp1 is overexpressed as previously postulated (9).

The importance of the residues mutated in *act1–102* for Scp1 binding was then tested *in vitro*. Actin was purified from yeast expressing wild-type or mutant *act1–102* actin (as described under "Experimental Procedures"). Recombinant Scp1 was purified from bacteria as previously described (5). Filamentous actin has been demonstrated to pellet at high *g*, and therefore, co-sedimentation of a protein to F-actin is widely used to demonstrate actin binding (see "Experimental Procedures"). Different concentrations of Scp1 (0.5–6.0 μM) were added to a constant concentration of F-actin (4.0 μM). After incubation, samples were centrifuged at high *g*. The resulting supernatants and pellets were run on gels, and these were analyzed using densitometry to determine the dissociation constant (K_d) of binding of Scp1 to the wild-type and mutant actins. The K_d of binding of Scp1 for *act1–102* was calculated to be 7.9 ± 2.2 μM, which is about 6-fold lower than the wild-type actin (1.3 μM ± 0.3).

Mapping the Sites of Actin Interaction in Scp1—In previous work we had demonstrated that Scp1 can bundle actin but itself was not a dimer (5). This suggested that Scp1 might carry 2 actin-binding sites. A series of Scp1 truncation mutants were generated as plasmid borne GFP fusions. Plasmids carrying these mutants were transformed into yeast cells, and localiza-
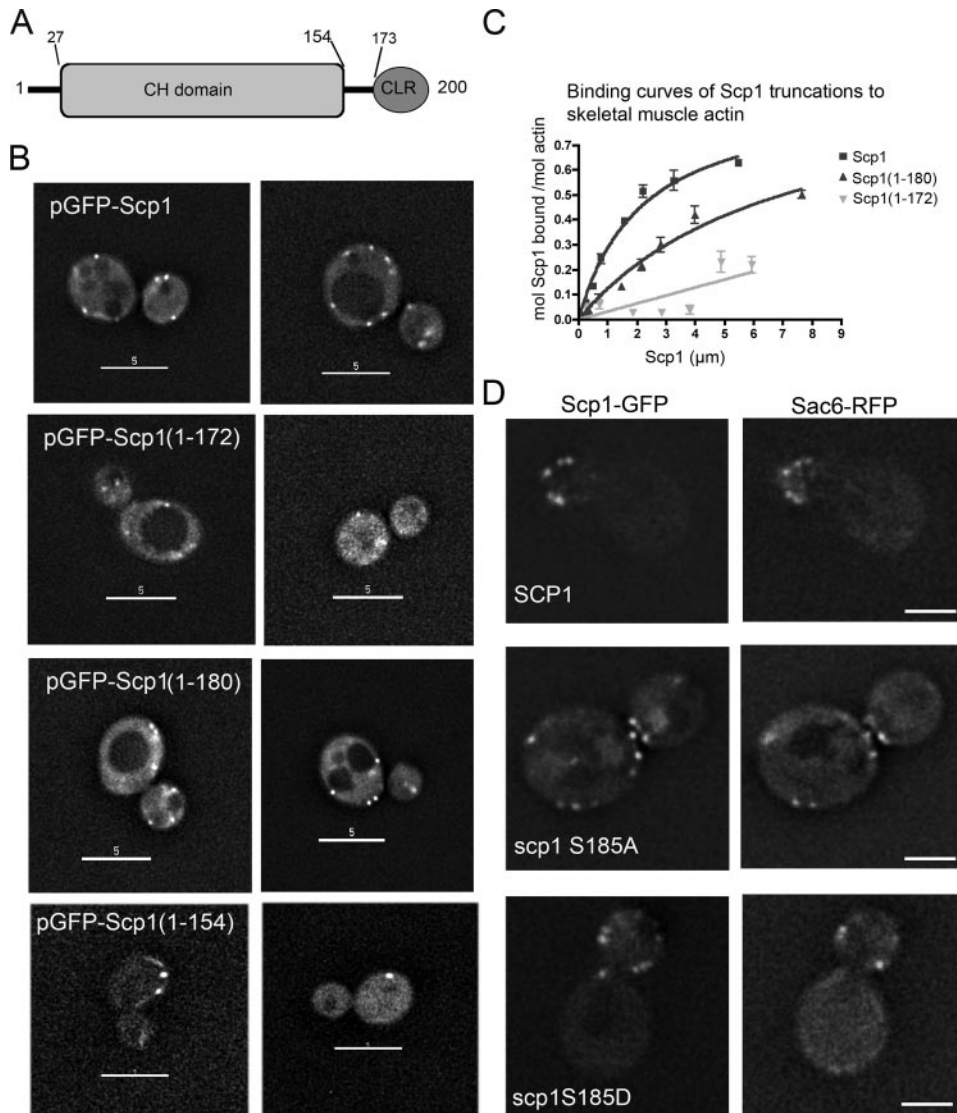
FIG. 4. **Expression of GFP-Scp1 mutants to map actin binding sites in Scp1.** *A*, schematic of Scp1 showing domain structure with a CH domain from residues 27–154 and a calponin like repeat (*CLR*) from 173 to 200. *B*, plasmid-borne GFP-Scp1 was mutated to generate truncations at residues 154, 172, and 180. These were expressed in cells. The Scp1-(1–154) showed no localization to actin structure. The Scp1-(1–172) and Scp1-(1–180) mutants showed localization but at a reduced level and with increased cytoplasmic staining compared with wild-type Scp1. *C*, binding affinities of His$_6$-Scp1-(1–172) and Scp1-(1–180) for rabbit skeletal muscle actin. Scp1-bound/mol actin was assessed using densitometry in four independent experiments. The binding curve for Scp1-(1–180) reveals a reduced affinity of this truncation for actin filaments, with a K_d value of 7.1 ± 2.5 μM (K_d for the full-length is 2.1 ± 0.4 μM). Stoichiometry of wild-type Scp1 and Scp1-(1–180) binding to actin were both ~1:1. The binding constant for Scp1-(1–172) to actin could not be calculated. *D*, GFP-Scp1 was also mutated to address the role of the putative phosphorylation site at position 185. Both mutants co-localized with Sac6-RFP, marking actin patches, and neither S185A nor S185D showed reduced localization, indicating that the phosphorylation of this site does not abrogate binding in either case.

ously been shown to not bind actin *in vitro* (5). The mutants Scp1-(1–172) and Scp1-(1–180) do show some spots, although these are fainter, and there appears to be increased cytoplasmic staining (Fig. 4*B*). This reduced staining of cortical patches may suggest that only one binding site may be present. This was tested *in vitro* by generating Scp1-(1–180) and Scp1-(1–172). As shown in Fig. 4*C*, Scp1-(1–180) has a K_d of 7.1 ± 2.5 μM compared with wild-type 2.1 ± 0.4 μM. The K_d for Scp1-(1–172), although clearly binding to actin, was too low to be calculated. Furthermore, in assays to measure actin bundling efficiency, actin bundling was not observed with the Scp1-(1–180) mutant (data not shown). *In vivo* assays of Scp1 mutants described in the next section also demonstrate the likely position of actin binding sites. Taken together these data strongly indicate that one binding site for actin lies at its extreme C terminus between residues 173 and 200 in the calponin-like repeat. The fact that localization is observed with Scp1-(1–172) but not with Scp1-(1–154) indicates the second binding site lies in the region 154–172.

A further point raised from other studies is the role of the putative Ser-185 phosphorylation site in Scp1. The mammalian homologue of Scp1, SM22, has been shown to be phosphorylated on the equivalent serine, Ser-181, and this phosphorylation reduces the actin binding capacity of the protein (25). It has been demonstrated that for Scp1 an S185D mutant behaves relatively normally *in vivo*, whereas the S185A mutant behaves more like a com-

tion was observed. Actin organization was determined in cells using rhodamine-phalloidin staining. In all cases, a wild-type pattern of cortical actin patches and actin cables was observed (data not shown). Fig. 4*A* shows the mutants generated within the known domain structure of Scp1. Scp1-(1–154) carrying only the CH domain did not show any detectable localization to cortical patches, suggesting it carries no actin binding sites as would be predicted for a single CH domain of this type (24) (Fig. 4*B*). The spots that were observed do not resemble the actin localization in these cells, which looks normal with multiple punctate spots (data not shown). This fragment had also previ-

plete deletion (4). We generated the GFP-Scp1 S185A and S185D mutants to determine whether the S185A mutant might have such a severe effect on function due to lack of localization to actin patches. However, as shown (Fig. 4*D*), both mutants co-localize to actin patches marked with Sac6-RFP, indicating that at least one actin binding site is functional in these mutants. It also strongly indicates that it is the bundling activity rather than binding that is regulated through this site.

Formation of Cortical Patches Is Defective in Actin-bundling Mutants—We and others have previously noted an overlapping function of the yeast fimbrin homologue Sac6 with Scp1 (4, 5).
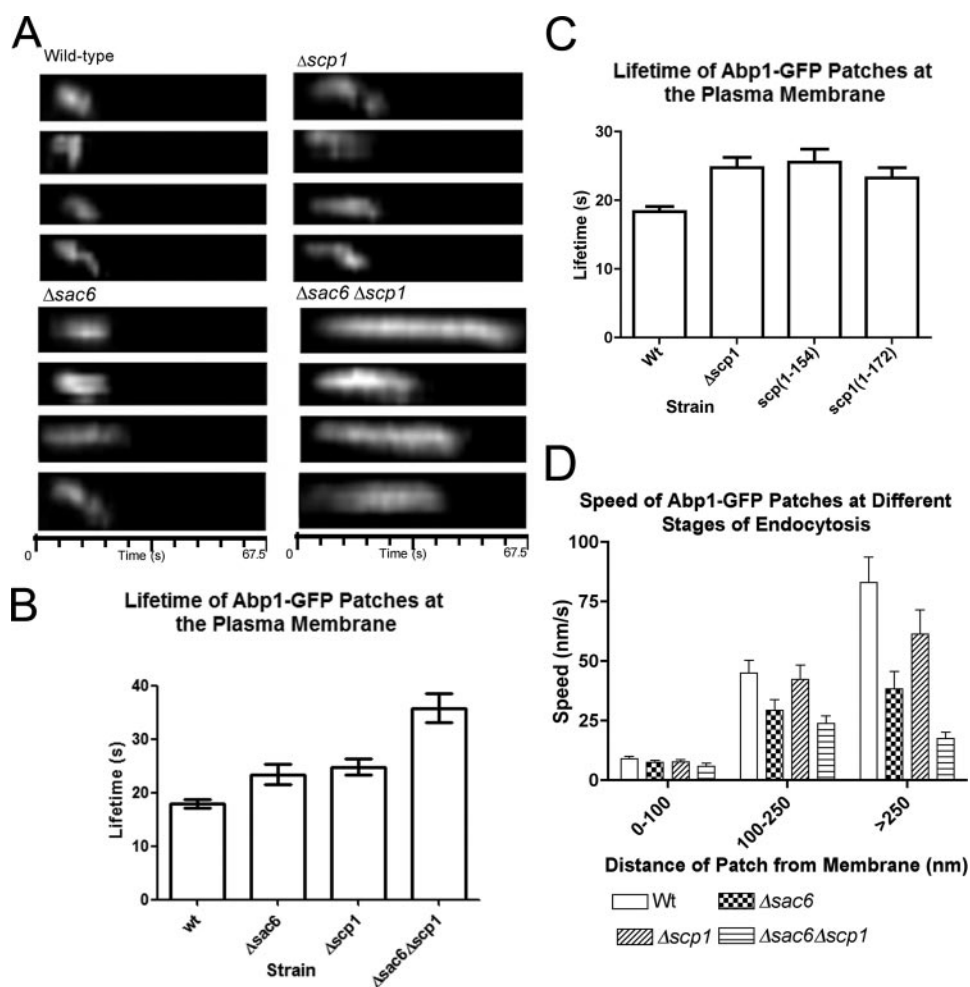
FIG. 5. **The behavior of Abp1-GFP in wild-type and mutant cells.** Abp1-GFP was expressed in wild-type cells and in mutants Δ*sac6*, Δ*scp1*, and Δ*sac6*Δ*scp1*. *A*, kymographs, 4 for each strain, depict behavior of patches over time at the plasma membrane. *B*, quantitation of multiple patches in wild-type (*wt*) Δ*sac6*, Δ*scp1*, and Δ*sac6*Δ*scp1* strains ($n > 25$) demonstrates that all mutants show increased lifetime at the plasma membrane. *t*-Tests show all strains are statistically distinct from wild-type ($p < 0.0001$). *C*, quantitation of multiple patches in strains in which *scp1* has been mutated, Scp1-(1–154) and Scp1-(1–172), and compared with wild-type and Δ*scp1* strains demonstrates that loss of bundling confers a null phenotype with respect to patch lifetime. $n > 25$. *t*-Tests show $p < 0.0001$ for wild type to Δ*scp1* and to Scp-(1–154) and $p < 0.0002$ for wild type to Scp-(1–172) comparison. *D*, assessment of distance moved over time was used to calculate speed of the patches in different strains at different stages of the endocytic process. All patches showed little movement within 100 nm of the membrane. Between 100 and 250 nm, the Δ*sac6* and Δ*sac6*Δ*scp1* strains showed a marked reduction in the rate of movement. In patches that moved over 250 nm, all mutants (Δ*sac6*, Δ*scp1*, and Δ*sac6*Δ*scp1*) showed a reduction in cortical patch rate of movement.

Deletion of *scp1* alone has no discernible effects on actin organization, whereas deletion of *sac6* alone has modest effects, and cells are still able to grow at broad range of temperatures. The combined deletion, however, has a severe growth phenotype, and cells are temperature-sensitive and have aberrant cortical actin structures (5).

The questions we have asked are, Why does the cell express two actin bundling activities that both function within the cortical patch, and also, Does deletion of *scp1* cause any detectable endocytic phenotype? GFP-Abp1 was used as a functional marker of actin patches forming during the endocytic process and was analyzed in wild type, Δ*sac6*, Δ*scp1*, and Δ*scp1*Δ*sac6* cells. Kymographs showing the behavior of representative patches are shown in Fig. 5*A*. The lifetime of the patches were also quantified (Fig. 5*B*). Deletion of either *sac6* or *scp1* increases patch lifetime from 17.9 to 23.4 or 24.7 s, respectively.

The double deletion showed an even more dramatic increase in lifetime to 35.8 s.

We also addressed the *in vivo* function of the Scp1 mutants Scp1-(1–154) and Scp1-(1–172). We reasoned that if *scp1* mutants have two actin binding sites, they should be able to bundle actin, and so cortical actin patches should behave in a similar way to wild type. If, however, bundling is defective and the mutants either do not bind or bind only one site, these patches should behave more akin to those in Δ*scp1* cells. Analysis of Abp1-GFP movement in cells expressing mutant Scp1 proteins was assessed. As shown (Fig. 5*C*) patches in these cells behave in a similar way to those in Δ*scp1* cells (lifetime: Scp1-(1–154), 25.5 ± 1.9 s; Scp1-(1–172), 23.2 ± 1.5 s), indicating that Scp1-(1–154) and Scp1-(1–172) are not functioning to bundle actin. However, because we see some cortical patch localization in Scp1-(1–172) (Fig. 4*B*), we can surmise that one binding site remains functional.

We also investigated the paths taken by the invaginating vesicles and their rate of movement (Fig. 5*D*). Initially, patches at the plasma membrane are relatively non-motile; there is then a slow inward movement that in wild-type cells occurs at 40 nm/s. This is followed by a fast movement of ≥80 nm/s. All stages of movement are impaired in the mutants, although the slow movement phase is not so greatly affected in the absence of *scp1*, suggesting that the most important role of Scp1 is at the later fast movement stage. Deletion of both bundling activities reduces the slow inward movement rate by 2-fold, whereas the fast movement stage is 5-fold slower. This demonstrates for the first time that bundling proteins play a key role not just at early stages of invagination but also at later stages, most likely after scission.

We then wanted to assess the proportion of the forming endocytic patches in the mutants that were able to enter the fast moving stage that usually occurs after about 250-nm movement from the membrane that is presumed to correspond to vesicles formed after scission (10, 26). This might be considered to indicate the proportion of vesicles that successfully form and enter the cell. As shown graphically in Fig. 6*A*, whereas wild-type and Δ*scp1* cells both showed >70% of patches able to enter the fast movement stage, only 40% of patches in Δ*sac6* cells moved past
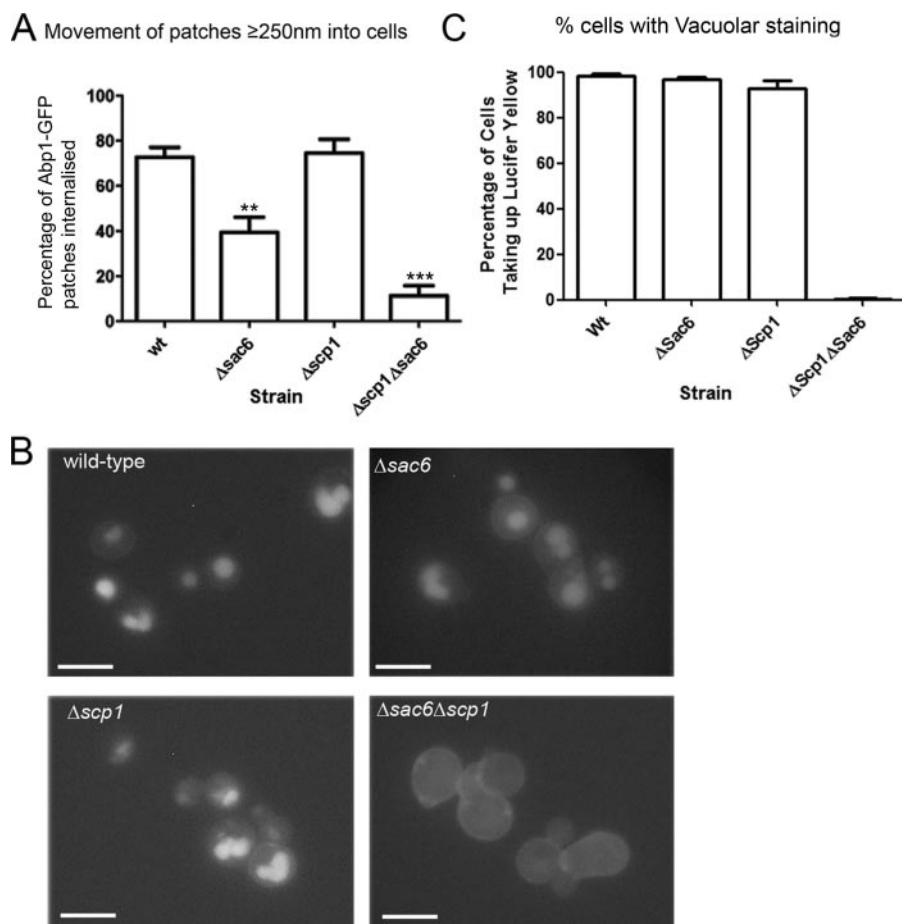
FIG. 6. **Deletion of bundling protein genes affects fluid phase endocytosis.** *A*, movement beyond 250 nm corresponds to initiation of fast movement of patches in wild-type (*wt*) cells presumably because vesicle scission has occurred. The number of patches moving past this point was assessed in all strains as an indication of successful endocytic events. *Error bars* are S.E. Statistical analysis used paired *t*-tests. Statistically relevant differences from wild type are indicated. **, *p* value ≤ 0.0025; ***, *p* value ≤ 0.0001. *B*, Lucifer yellow uptake was monitored in wild-type cells and in mutants Δ*sac6*, Δ*scp1*, and Δ*sac6*Δ*scp1*. *Bar*, 5 μm. *C*, these data were quantitated and shown graphically. Wild-type and the single mutants all showed uptake of the fluid phase marker into vacuoles in >90% of cells. However, the double deletion strain Δ*sac6*Δ*scp1* showed almost complete absence of uptake, indicating a severe endocytic defect (wild type, *n* = 212; Δ*sac6*, *n* = 331; Δ*scp1*, *n* = 374; Δ*sac6*Δ*scp1*, *n* = 112).

to bind along the length of actin filaments (rather than at either end (27)). Thus, the intensity of GFP-Abp1 is likely to indicate the accessibility of Abp1 binding sites within the patch. Intriguingly, the fluorescence intensity of cortical patches was significantly reduced in the Δ*sac6* cells even though these patches had a longer lifetime than those in wild-type cells. The intensity of the patches in the wild-type, Δ*scp1*, and Δ*sac6*Δ*scp1* strains was about equal (Fig. 7*A*). These data indicate that in the absence of Sac6, there are fewer sites for Abp1 binding, resulting in lower intensity of patches. This change could be brought about if Scp1 partly functioned in place of Sac6 and if Scp1 interacted with actin in a different way to Sac6 to generate tighter bundles that are less accessible to Abp1 binding.

We also asked whether the reason that the single mutants had relatively minor phenotypes compared with the double deletion could in part be due to a compensatory increased level of one protein in the absence of the other. We made extracts of cells that were wild type or deleted for one or both proteins. These were then separated by SDS-PAGE and Western-blotted. The blots were probed with antibodies to Sac6 or Scp1. As shown in Fig. 7*B*, deletion of *sac6* causes an increase

250 nm into the cell. The loss of both bundling activities severely compromised inward movement with less than 10% of patches moving over 250 nm into the cell. We then determined the effect of the deletions on endocytosis of the fluid phase marker Lucifer yellow. Mutants were incubated for 80 min with Lucifer yellow and then analyzed by fluorescence microscopy (Fig. 6*B*). Staining of vacuoles can be clearly visualized for both wild type and the single mutants. Thus, although the Δ*sac6* cells show marked defects in movement of patches, the cells can still endocytose fluid phase markers sufficiently to be clearly visualized in this assay. In contrast, the Δ*sac6*Δ*scp1* cells show no obvious staining of the vacuole, reflecting the very low proportion of endocytic patches that were detected as moving into the cell.

Patches Containing Only Scp1 Are Distinct from Patches in Wild-type Cells—Although our data show that Scp1 has a greater influence later in the endocytic process than Sac6, we also wanted to address the mechanistic differences between the cellular roles of Sac6 and Scp1. To investigate this we measured the intensity of forming Abp1-GFP patches. Abp1 is proposed

in the level of Scp1 in cells. This was quantified over three independent experiments, and data demonstrate an increase of about 50% in Scp1 levels in the absence of Sac6. The converse was also observed, with an increase in Sac6 protein of about 30% in cells that were deleted for *scp1*. Thus, cells appear to have mechanisms to compensate for the loss of bundling activity.

If the actin associated with the invaginating vesicle membrane is no longer tightly bundled, this might be expected to impact on the patch morphology. To address this, cortical patch diameters were measured as described under "Experimental Procedures" in the wild-type, Δ*scp1*, Δ*sac6*, and Δ*sac6*Δ*scp1* strains. As shown in Fig. 7*C*, whereas patches in wild-type and Δ*scp1* strains are very consistent in their diameter (208 and 210 nm, respectively), lack of *sac6* causes the patches to increase in diameter to about 305 nm), and the lack of any actin-bundling activity produces a much larger size patch with a diameter almost double that of the wild-type cells (415 nm).

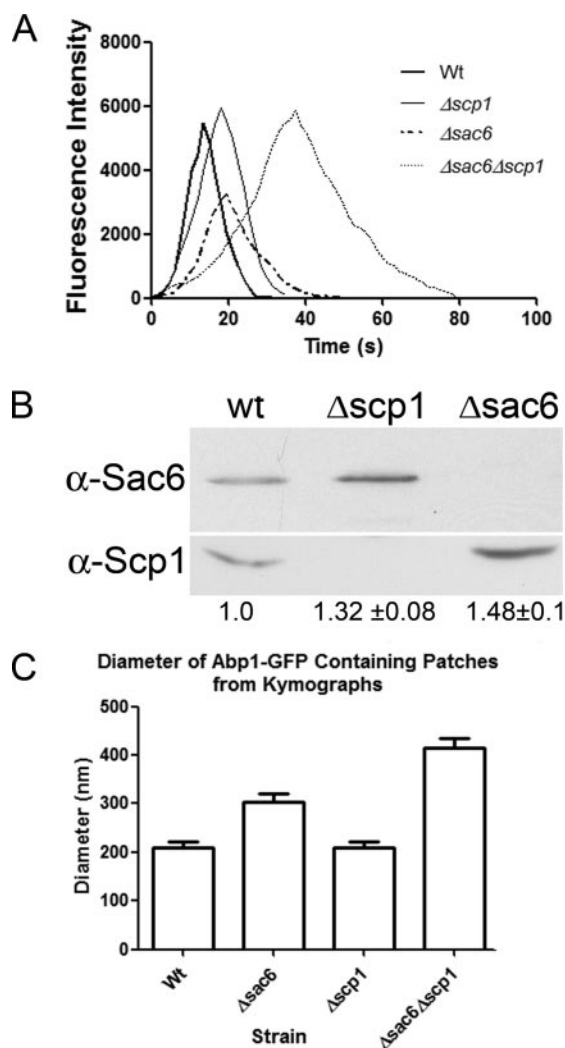*Scp1 Is Recruited to Cortical Patches Later Than Sac6*—Our data in Fig. 5 suggests that deletion of *sac6* has an effect on the

FIG. 7. **Differences between Δ*sac6* and Δ*scp1* cells indicate different modes of interaction with actin.** *A*, average cortical patch intensities were assessed for wild-type (*wt*) cells and in mutants Δ*sac6*, Δ*scp1*, and Δ*sac6*Δ*scp1* for >18 patches. In the absence of *sac6*, but not in wild type or in the mutants lacking Δ*scp1*, the maximum intensity of the patch was by >40%. *B*, the cell compensates for lack of actin-bundling proteins. In cells lacking Δ*scp1* there is a measurable increase in the level of Sac6 protein as detected by Western blotting, whereas in the absence of Δ*sac6* there is an increase in the level of Scp1 protein. These data are the average of three independent repetitions of the protein extract preparation and Western blotting. *C*, the diameter of Abp1-GFP patches in wild-type and mutant strains were measured from kymographs as described under "Experimental Procedures." For each strain $n \geq 25$. All strains show statistically relevant differences in *t*-tests with *p* values of ≤ 0.0005.

invagination stage of endocytosis, whereas *scp1* deletion only affects the final, inward movement stage. Temporal control of endocytic complex assembly is likely to be important for ensuring that appropriate structures formed at the right time. To investigate the timing of recruitment of Scp1 and Sac6, we generated strains containing both Sac6 fused to an mRFP tag and Scp1 fused at the N or C terminus with GFP. Sac6-mRFP is considered to be a fully functional protein, as its expression in the absence of endogenous Sac6 behaves as a wild-type cell rather than exhibiting phenotypes associated with the *SAC6* deletion. Scp1 fused to GFP at its N or C terminus generates a protein that co-localizes to actin patches. However, neither of the Scp1 fusions is fully functional, as the phenotype of a Δ*sac6*

Scp1GFP strain is more compromised than the *sac6* deletion alone (data not shown). Because the fusions localize appropriately, we still considered that meaningful data could be obtained by comparison of these fusions and that currently these approaches provide the best means to gain insights into spatiotemporal aspects of endocytic complex formation in cells. First, we measured the lifetime of all three fusions. As shown in Fig. 8*A*, Sac6 lifetime is 16.15 ± 0.46 s. This is slightly shorter than that of Abp1 in our cells. Sac6 lifetime is, however, longer than that of Scp1. Interestingly, the lifetime of both N-terminal-tagged Scp1 (11.8 ± 0.8 s) is almost identical to that of the C-terminal-tagged protein (11.6 ± 1.0 s). Thus, the Scp1 fusion protein can localize correctly within the cell and has a lifetime appropriate for its incorporation into actin patches.

We then determined the relative time of recruitment for each protein. We have analyzed the N-terminal-tagged GFP-Scp1 because this fusion is furthest from the actin binding site and so potentially less likely to interfere with this function. By imaging the fusions proteins simultaneously, we could determine that Sac6 arrives at the forming endocytic patch 1.2 s before Scp1 and leaves 1.6 s after. Intensity profiles and distance plots were then generated for both Sac6-mRFP and GFP-Scp1 following four spots for each protein (Fig. 8, *B* and *C*). Co-localization of sac6RFP and GFP-Scp1 is shown in Fig. 8*D*. These data show that Sac6 localizes to spots at the plasma membrane, reaching its greatest intensity just before movement away from the plasma membrane. GFP-Scp1 shows a broader distribution of intensities. On average, the greatest intensity is reached just at or after movement from the membrane has been initiated. This agrees with our data above that the lifetime of Scp1 is shorter and that it arrives after Sac6.

DISCUSSION

Recent studies have given us a framework to begin to understand the process of endocytosis. However, although distinct stages of endocytosis have been determined, the role of many of the proteins that localize to the cortical complexes is largely unknown. Central to endocytosis in yeast is the polymerization and turnover of F-actin. Cells that have a disassembled actin cytoskeleton due to treatment with the drug latrunculin-A or that have a stabilized actin cytoskeleton that cannot disassemble after jasplakinolide addition cannot perform endocytosis (19, 28). Other studies have highlighted the importance of actin depolymerization by cofilin and actin nucleation by Arp2/3 and the WASP homologue Las17 (29–31). However, it is not simply assembly and disassembly of actin filaments that appears to be important for endocytosis. The ability to generate higher order structures in the form of bundles has also been demonstrated to be significant (10). Sac6 is the homologue of mammalian fimbrin and is known to bundle actin *in vitro* (6). A second bundling protein, Scp1, the homologue of mammalian SM22, is also known to localize to patches, but its deletion does not confer obvious defects in actin organization or in fluid phase endocytosis (4, 5). In this study we addressed two key questions. First, does the actin-bundling protein Scp1 serve a distinct function from Sac6? Second, what is the overall contribution of the bundling proteins Sac6 and Scp1 to the endocytic process?
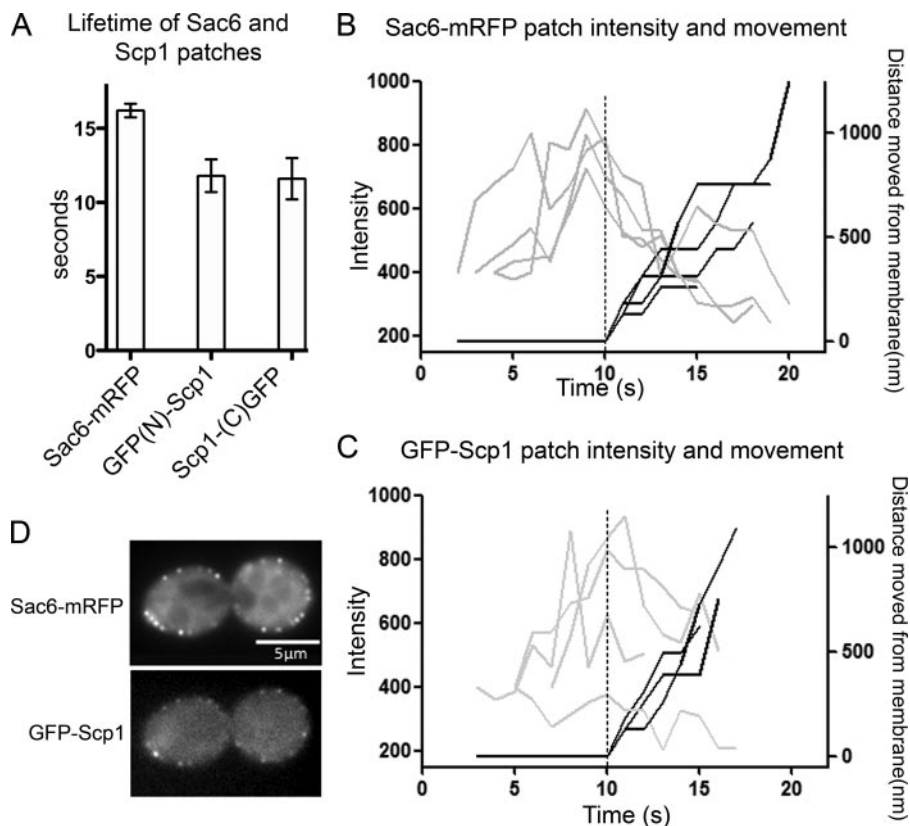
FIG. 8. **Sac6 and Scp1 dynamics in endocytic patches.** *A*, lifetimes of individual sac6-mRFP or GFP-Scp1 patches ± S.E. in wild-type and mutant cells. $n > 37$ patches for each strain. Movies were taken with 1-s frame intervals for both Sac6-mRFP and GFP-Scp1. For Sac6-mRFP (*B*) and GFP-Scp1 (*C*), fluorescence intensity (*gray*) and distance from site of patch formation (*black*) were measured as a function of time. Each line represents data from one patch. Fluorescence intensity over time was corrected for photobleaching. *D*, images showing co-localization of Sac6-mRFP and GFP-Scp1 in cells. *Bar* = 5 μm.

initiated, whereas Scp1 is more constant or increasing at this time. This might suggest that Scp1 is able to compete Sac6 from the actin filaments. Competition for F-actin binding between Sac6 and Scp1 was shown *in vitro* previously (4).

Our *in vitro* data allows us to consider these differences further. These studies indicate that Scp1 binds strongly to pre-polymerized actin filaments and binds mature filaments, possibly that could already be bundled and stabilized by Sac6p. Analysis of the intensity of GFP-Abp1 localization at cortical patches is likely to reflect the binding sites available on F-actin for binding. One observation was the sharp drop in intensity of the patches in the *sac6* null cells. In these cells we also know that there is an increase in the level of Scp1 (Fig. 7). This would suggest that Scp1 bundles actin more tightly than Sac6, thus reducing the availability of binding sites for Abp1. The idea of tight bundling by Scp1 is supported by previous data from our laboratory, where actin bundles formed in the presence of Scp1 were visualized by electron microscopy

Tracking of GFP-Abp1 patches in Δ*sac6* cells has previously indicated that patches show little directed movement, and the model proposed suggests that Sac6 bundles actin to provide a strong framework to allow sufficient force to be generated to allow the vesicles to be drawn into the cell (10). We compared characteristics of GFP-Abp1 movement in cells lacking either *sac6* or *scp1* or both. Key findings were that patches in both *sac6* and *scp1* had a longer lifetime than wild-type cells, so this makes it likely that both contribute to the bundling process necessary for directed inward movement of vesicles. Second, deletion of *sac6* had a more marked effect on the speed of vesicle movement both at the invagination (slow) stage of patch movement and at the post-scission (fast) stage of movement. Deletion of *scp1* had a more marked effect at this later stage, with little impact on the slow movement. This is the first evidence for a mechanistic difference in the function of these proteins. The measurement of patch diameters supports this idea. We suggest that the patch diameter measured at the point immediately before movement of the membrane is a measurement of actin organization at this early stage of endocytosis. Deletion of *sac6*, which we propose functions early in invagination, has a more marked effect on diameter than does deletion of *scp1* (Fig. 7*C*). We also demonstrate in Fig. 8 that Scp1 is recruited to cortical patches after Sac6, demonstrating temporal organization in actin bundling activities at the endocytic site. Interestingly, the Sac6 intensity in the patch decreases rapidly after movement is

(5). In the study here we have shown that there are two binding sites for Scp1 on actin and that these lie relatively close together in the C-terminal portion of Scp1. Given that these regions will contact distinct filaments to cause bundling and that Scp1 itself is only 22.7 kDa, it would be expected that the filaments in the bundle will be tightly packed. This would be in contrast to Sac6, which is much larger (71.7 kDa) and so will occupy a larger space between filaments and would, therefore, bundle less tightly.

In support of the idea that Scp1 bundles actin more tightly, we cannot observe any staining by immunofluorescence microscopy of Scp1, but we can for Sac6 (Fig. 2).[6] We consider it likely that cross-linking in cells during fixation by formaldehyde might make it impossible for the antibodies to access Scp1 bundled between actin filaments. Another possibility for the lack of staining, however, could be that the primary epitope in our antibodies is against the actin:Scp1 interface. Furthermore, Sac6 can be functionally tagged by GFP and RFP insofar as the fusions do not compromise the cell growth as does a *sac6* deletion and that the kinetics of Sac6RFP movement in our hands closely resemble those of Abp1-GFP (Fig. 8). On the other hand, neither N- or C-terminal GFP tagging of Scp1 generates a fully functional protein as indicated by reduced growth in the Δ*sac6*

background. The fusion protein does, however, localize to endocytic patches, and its lifetime in the patches is appropriate for the function of the protein. Our data indicate that the fusion of the GFP moiety, which is larger than Scp1, may preclude binding in the normal way within the core of tight bundles. Most likely GFP-Scp1 is able to bind to the outer filaments in a bundle, as we can see protein localization, but the GFP will sterically block the ability of Scp1 to bundle in the normal fashion.

All these data together indicate that Scp1 functions to bundle actin tightly at a late stage in endocytosis to assist the effective inward movement of the vesicle. We propose a model in which Sac6 would serve an initial bundling function to provide a framework to support the invagination process. Scp1 would then bundle these filaments more tightly to generate a more rigid support to allow the directed inward movement of the vesicles. Thus, in the absence of *sac6* alone, there is more haphazard movement initially, and some patches disassemble without ever showing fast movement, but the increase in Scp1 levels (Fig. 7) is sufficient to still allow a significant number of patches to fully endocytose into the cell. In the absence of *scp1*, many patches behave relatively normally, but these have a longer lifetime, in part due to their slower movement at later stages of the endocytic process, suggesting that Sac6 does not fully compensate for loss of *scp1* at this stage. Finally, in the double deletion we observe only a small number of endocytic events that culminate in inward movement into the cell and a correspondingly low level of fluid phase endocytosis.

We conclude that both Sac6 and Scp1 function to generate the rigid actin framework that is required for the invagination process that takes place during endocytosis. However, our evidence demonstrates that they interact in different ways with actin and that Scp1 is likely to form tighter bundles that are most important for later stages of endocytosis. The importance of actin bundling to the cell is further reflected in the fact that a compensatory mechanism functions to increase levels of one protein when the other is absent.

REFERENCES

1. Moseley, J. B., and Goode, B. L. (2006) *Microbiol. Mol. Biol. Revs.* **70,** 605–645
2. Smythe, E., and Ayscough, K. R. (2006) *J. Cell Sci.* **119,** 4589–4598
3. Toret, C. P., and Drubin, D. G. (2006) *J. Cell Sci.* **119,** 4585–4587
4. Goodman, A., Goode, B. L., Matsudaira, P., and Fink, G. R. (2003) *Mol. Biol. Cell* **14,** 2617–2629
5. Winder, S. J., Jess, T., and Ayscough, K. R. (2003) *Biochem. J.* **375,** 287–295
6. Adams, A. E. M., Botstein, D., and Drubin, D. G. (1991) *Nature* **354,** 404–408
7. Drubin, D. G., Miller, K. G., and Botstein, D. (1988) *J. Cell Biol.* **107,** 2551–2561
8. Kübler, E., and Riezman, H. (1993) *EMBO J.* **12,** 2855–2862
9. Gourlay, C. W., Carpp, L. N., Timpson, P., Winder, S. J., and Ayscough, K. R. (2004) *J. Cell Biol.* **164,** 803–809
10. Kaksonen, M., Toret, C. P., and Drubin, D. G. (2005) *Cell* **123,** 305–320
11. Kaiser, C., Michaelis, S., and Mitchell, A. (1994) *Methods in Yeast Genetics: A Laboratory Course Manual*, Cold Spring Harbor Laboratory Press, Cold Spring Harbor, NY
12. Longtine, M. S., McKenzie, A., Demarini, D. J., Shah, N. G., Wach, A., Brachat, A., Philippsen, P., and Pringle, J. R. (1998) *Yeast* **14,** 953–961
13. Moseley, J. B., Maiti, S., and Goode, B. L. (2006) *Methods Enzymol.* **406,** 215–234
14. Winder, S. J., Hemmings, L., Maciver, S. K., Bolton, S. J., Tinsley, J. M., Davies, K. E., Critchley, D. R., and Kendrick Jones, J. (1995) *J. Cell Sci.* **108,** 63–71
15. Hettema, E. H., and Ayscough, K. R. (2007) in *Yeast Gene Analysis* (Stansfield, I., and Stark, M. J. R., eds) 2nd Ed., pp. 241–268, Elsevier, Oxford, UK
16. Hagan, I. M., and Ayscough, K. R. (2000) in *Protein Localization by Fluorescence Microscopy: A Practical Approach* (Allan, V. J., ed) pp. 179–206, Oxford University Press, New York
17. Dulic, V., Egerton, M., Elgundi, I., Raths, S., Singer, B., and Riezman, H. (1991) *Methods Enzymol.* **194,** 697–710
18. Ayscough, K. R., Stryker, J., Pokala, N., Sanders, M., Crews, P., and Drubin, D. G. (1997) *J. Cell Biol.* **137,** 399–416
19. Holtzman, D. A., Wertman, K. F., and Drubin, D. G. (1994) *J. Cell Biol.* **126,** 423–432
20. Honts, J., Sandrock, T., Brower, S., O'Dell, J., and Adams, A. (1994) *J. Cell Biol.* **126,** 413–422
21. Belmont, L. D., Patterson, G. M., and Drubin, D. G. (1999) *J. Cell Sci.* **112,** 1325–1336
22. Holmes, K. C., Popp, D., Gebhard, W., and Kabsch, W. (1990) *Nature* **347,** 44–49
23. Kudryashov, D. S., Sawaya, M. R., Adisetiyo, H., Norcross, T., Hegyi, G., Reisler, E., and Yeates, T. O. (2005) *Proc. Natl. Acad. Sci. U. S. A.* **102,** 13105–13110
24. Gimona, M., and Winder, S. J. (1998) *Curr. Biol.* **8,** 674–675
25. Fu, Y. P., Liu, H. W., Forsythe, S. M., Kogut, P., McConville, J. F., Halayko, A. J., Camoretti-Mercado, B., and Solway, J. (2000) *J. Appl. Physiol.* **89,** 1985–1990
26. Liu, J., Kaksonen, M., Drubin, D. G., and Oster, G. (2006) *Proc. Natl. Acad. Sci. U. S. A.* **103,** 10277–10282
27. Goode, B. L., Rodal, A. A., Barnes, G., and Drubin, D. G. (2001) *J. Cell Biol.* **153,** 627–634
28. Ayscough, K. R. (2000) *Curr. Biol.* **10,** 1587–1590
29. Lappalainen, P., and Drubin, D. G. (1997) *Nature* **388,** 78–82
30. Madania, A., Dumoulin, P., Grava, S., Kitamoto, H., Scharer-Brodbeck, C., Soulard, A., Moreau, V., and Winsor, B. (1999) *Mol. Biol. Cell* **10,** 3521–3538
31. Winter, D., Lechler, T., and Li, R. (1999) *Curr. Biol.* **9,** 501–504